Concurrent wind and base vibration energy harvesting with a broadband bistable aeroelastic energy harvester

IOP Conf. Series: Materials Science and Engineering **531** (2019) 012081 doi:10.1088/1757-899X/531/1/012081

Concurrent wind and base vibration energy harvesting with a broadband bistable aeroelastic energy harvester

Liya Zhao*

School of Mechanical and Mechatronic Engineering, Faculty of Engineering and Information Technology, University of Technology Sydney, 15 Broadway Ultimo 2007, NSW, Australia

*Email: liya.zhao@uts.edu.au

Abstract. This paper presents a novel energy harvesting device driven by concurrent aeroelastic vibration and base vibratory excitation. The harvester undergoes flow-induced limit-cycle oscillation under galloping instability, and at the same time, inertia force induced vibration is present due to the base vibratory excitation. A limitation with a traditional linear aeroelastic energy harvester is that effective energy harvesting from combined sources is only achievable within a narrow frequency range. To overcome this issue, bistability is introduced by exploiting nonlinear restoring force. A lumped aero-electro-mechanical model is established to incorporate the mutual coupling between the wind flow, piezoelectric element, nonlinear structure and circuit. Dynamic responses are investigated for different bistable configurations. Results show that the proposed harvester achieves a significantly widened bandwidth over which the two excitation frequencies are forced to lock into each other, and both vibratory and aeroelastic energy are effectively harnessed.

1. Introduction

The development of ultralow-power electronics arouses the research enthusiasm in harvesting small-scale renewable energy to implement perpetually self-powered microelectronic devices, such as wireless sensors. Possible renewable sources surrounding such devices include vibration, solar energy, wind energy, thermal energy, etc. Among them, wind energy is a ubiquitous source in both outdoor and indoor environments, like the bridges, HVAC systems, and so on. Development of rotary-type turbines for large-scale wind energy conversion is quite mature. However, their efficiency is greatly lowered when miniaturized or when strong wind is not available. In the recent years, researchers have investigated new concepts for small-scale wind energy harvesting by exploiting aeroelastic instabilities. Various aeroelastic energy harvesters have been proposed based on aeroelastic phenomena, such as vortex-induced vibrations (VIV) of cylinders [1], modal convergent flutter of flapping airfoils [2], galloping of prisms with certain cross-section shapes, like square, D-shape and triangle [3,4], and wake galloping of parallel cylinders [5]. Researchers have also proposed various methods to reduce the onset wind speed threshold and enhance wind power extraction efficiency. Efforts include modifying circular cylinder cross-section of a VIV energy harvester by Hu et al. [6], employing a 2DOF cut-out structure for a galloping harvester by Zhao et al. [7], adding a beam stiffener as an electromechanical coupling booster by Zhao and Yang [8], etc. Moreover, nonlinear interface circuits based on synchronous switching techniques have also been investigated to improve wind energy harvesting [9].

There are a broad range of situations where two or more sources are coexisting. For example, on vehicles, railway tracks, ocean buoys, ships, aircrafts, etc., both wind flows and mechanical vibrations are present. However, it appears very few studies to date have investigated concurrent energy harvesting to simultaneously scavenge wind and base vibratory energy. Bibo and Daqaq [2] reported to use a single aeroelastic flutter energy harvester to harvest combined loadings, and achieved enhanced power output when the base excitation frequency is close to the harvester's resonance. However, the harvester is extremely susceptible to a reduction in power output if a slight frequency mismatch occurs. Outside the narrow range near resonance, two concurrent excitation frequencies couple in a way to induce quasi-periodic oscillations, hampering effective energy harvesting from combined sources. This problem is also observed in concurrent energy harvesting using VIV and galloping harvesters [10,11]. In the field of vibration energy harvesting, considerable efforts have been reported to broaden the bandwidth, such as monostable, bistable or tristable designs, multi-modal techniques, frequency up-conversion or impact-based designs [12-15]. These techniques have great potential to enhance concurrent energy harvesting. However, incorporating these techniques will complicate the multi-way coupling between the structure, piezoelectric element, circuit, wind flow and vibratory excitation force. Their effectiveness and the associated dynamic responses should be carefully examined. Recently, Zhao and Yang [16] and Zhao [17] successfully achieved wideband concurrent energy conversion with an impact-based piecewise-linear configuration based on galloping.

This paper proposes a new device to concurrently harness coexisting aeroelastic and vibratory energy by incorporating the concepts of galloping aeroelasticity and nonlinear bistability. The aim is to explore the potential benefits in broadening the bandwidth over which the two sources are simultaneously harnessed by locking-in and supplementing each other.

2. Energy Harvesting Principle

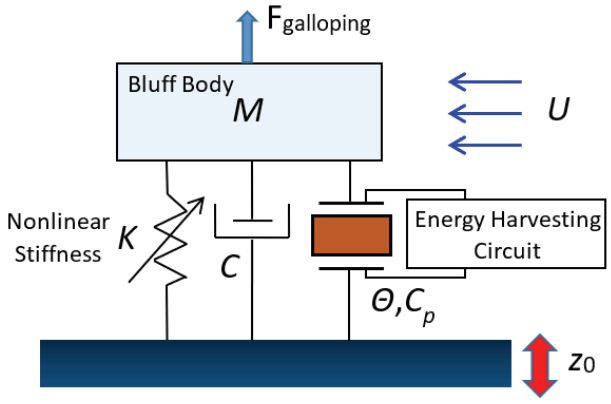

Figure 1. Diagram of the proposed bistable concurrent aeroelastic and vibratory energy harvester

The diagram of the proposed energy harvesting device is shown in Figure 1. The harvester consists of a flexibly supported bluff body coupled to a power extraction circuit through a vibration-electricity transduction mechanism, which is the piezoelectric transduction employed here. M is effective mass of the harvester, Θ is the lumped electromechanical coupling, and C_p is the piezoelectric capacitance. The bluff body is exposed to incident wind with a speed $\overline{U}$. When $\overline{U}$ exceeds the cut-in speed $\overline{U}_{cr}$, the destabilizing negative damping effect of the aerodynamic force overcomes the stabilizing inherent mechanical damping C, giving rise to self-excited transverse galloping oscillation in the direction normal to the wind. The oscillation amplitude exponentially increases until the positive aerodynamic nonlinearity is large enough to bring the overall damping back to zero and create limit-cycle oscillations with constant amplitude. The bluff body should be with certain cross-sections that satisfy

Den Hartog stability criteria [18], such as square, rectangle, triangle, D-shape, etc. Beside wind excitation, the harvester oscillator is subject to base excitation $\bar{z}_0 = Zcos(\omega t)$, where Z is the amplitude and ω is the base excitation frequency. The system stiffness K is nonlinear providing a nonlinear restoring force. which makes the two excitation sources nonlinearly coupled. A bistable restoring force is exploited here, with which the potential energy is double-well with two stable equilibriums. With the wind excitation, it is easy to induce inter-well large amplitude oscillations, coupling the two energy sources over a wide frequency range.

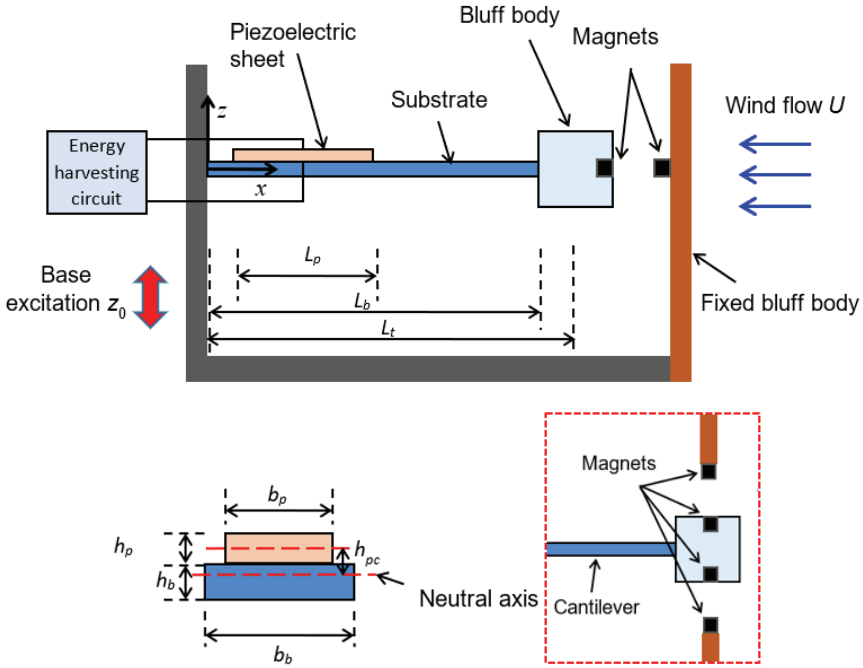

Figure 2. Schematic of the conceived practical design

A conceived practical design of the proposed device is shown in Figure 2. It consists of a bluff body with properly chosen cross-section connected to the free end of a cantilever. A piezoelectric element is bonded near the fixed end of the cantilever to convert the strain energy into electricity. The piezoelectric electrodes are connected to energy harvesting circuit to extract the generated power. To induce the nonlinear stiffness, magnetic interaction is employed. A magnet is embedded into the bluff body, and another is attached to a fixed rigid prism. Since the windward prism will make the flow turbulent, the section of bluff body should be able to undergo self-excited galloping in turbulent flow condition, for example, the D-shape. If the device is to be utilized in smooth flow condition, the magnets can be arranged in a way as shown in the bottom of Figure 2. Four magnets are used to ensure mass distribution symmetry. Square section, for example, can be utilized in such a case.

3. Analytical Model

The aero-electro-mechanically coupled model for the concurrent energy harvester is given by

$$M\ddot{\bar{u}} + C\dot{\bar{u}} + K_0\bar{u} + F_{nl} + \Theta\bar{V} = F_{air} - M\ddot{\bar{z}}_0 \tag{1}$$

$$\bar{I} + C_p\dot{\bar{V}} - \Theta\dot{\bar{u}} = 0 \tag{2}$$

where K_0 is the effective stiffness of the initial linear structure, F_{nl} is external nonlinear restoring force, F_{air} is the aerodynamic galloping force, $\bar{u}$ is the relative displacement of the bluff body to the base, $\bar{V}$

is the voltage across the piezoelectric electrodes, and $\bar{I}$ is the electrical current flowing into the circuit. The overdot denotes a derivative with respect to time t. A simple resistor R is considered in the circuit in this study, thus I is calculated by $\bar{I} = \bar{V}/R$. F_{air} is modeled based on the quasi-steady hypothesis, given by

$$F_{air} = \frac{1}{2}\rho h L \bar{U}^2 \left[\sum_{i=1}^{3} A_i \left(\frac{\dot{\bar{u}} + \dot{\bar{z}}_0}{\bar{U}} \right)^i \right] \tag{3}$$

where ρ, h, L and A_i are the air density, frontal height and length of the bluff body, and empirical aerodynamic coefficients, respectively. F_{nl} is taken to be in a cubic polynomial form, given by

$$F_{nl} = -\alpha \bar{u} + \beta \bar{u}^3 \tag{4}$$

where α and β are positive real numbers. If $K_0 < \alpha$, the system will be bistable. Equations (1) and (2) can be nondimensionalized as

$$\ddot{u} + 2\zeta \dot{u} + k_1 u + k_3 u^3 + \kappa_e v = -\ddot{z}_0 + \frac{U^2}{2m} \left[\sum_{i=1}^{3} A_i \left(\frac{\dot{u} + \dot{z}_0}{U} \right)^i \right] \tag{5}$$

$$\frac{v}{r} + \dot{v} - \dot{u} = 0 \tag{6}$$

with the dimensionless parameters defined by

$$u = \frac{\bar{u}}{h},\ z_0 = \frac{\bar{z}_0}{h},\ v = \frac{C_p \bar{V}}{\Theta h},\ m = \frac{M}{\rho h^2 L},\ U = \frac{\bar{U}}{\omega_n h},\ \Omega = \frac{\omega}{\omega_n},\ r = C_p R \omega_n,\ \tau = \omega_n t,\ \omega_n = \sqrt{\frac{K}{M}},$$
$$\zeta = \frac{C}{2M\omega_n} \quad k_1 = 1 - \frac{\alpha}{K},\ k_3 = \frac{\beta h^2}{K} \tag{7}$$

The overdot in Equations (5) and (6) denotes a derivative with respect to dimensionless time.

4. Results and discussion

The responses of the linear galloping energy harvester are first characterized based on Equations (5) and (6), with k_1=1 and k_3=0. Other system parameters are ζ=0.011, r=0.91141, κ_e=0.011359, m=57.58, A_1=2.3, A_2=0 and A_3=-18. If the base excitation amplitude Z is set to 0, it degrades to pure galloping condition, while if the wind speed U is set to 0, it is pure base vibration energy harvesting. The predicted responses of dimensionless average power p_{ave} under pure galloping and pure base vibration conditions for the linear harvester are shown in Figure 3 (a) and (b). p_{ave} is calculate by $p_{ave}=v_{rms}^2/r$. Figure 3(a) shows that below U_{cr}=1.408, i.e., the cut-in speed, the harvester is not able to extract wind power due to the inherent mechanical damping. Beyond this threshold speed, p_{ave} increases monotonically with increasing U. This characteristic of being able to generate power in an infinite range of wind speed is a great advantage of galloping for energy harvesting. A linear response with the peak p_{ave} at resonance around Ω=1 is seen in Figure 3(b) with an RMS base acceleration a_{rms} of 0.005. Figure 3(c) shows the variation of p_{ave} as a function of Ω under combined wind and base vibration sources with U=2.347 and a_{rms}=0.005. It is seen that the curve of p_{ave} when Ω is away from 1, i.e., the resonance, is flat, with a level approaching that from pure galloping. This indicates that in these regions, base vibration energy is not effectively harnessed. When Ω approaches 1 from the left side, a

deep valley occurs where p_{ave} drops to a minimum. When Ω is close to 1, p_{ave} reaches a peak, where wind and base vibration sources supplement each other to achieve effective concurrent energy harvesting. In all three figures, the optimal resistance r_{opt} is used. The bandwidth of concurrent energy harvesting is defined in this study to be the range of frequency over which p_{ave} is higher than that from pure galloping. It is apparent that a linear galloping energy harvester provides a very narrow bandwidth under concurrent loadings.

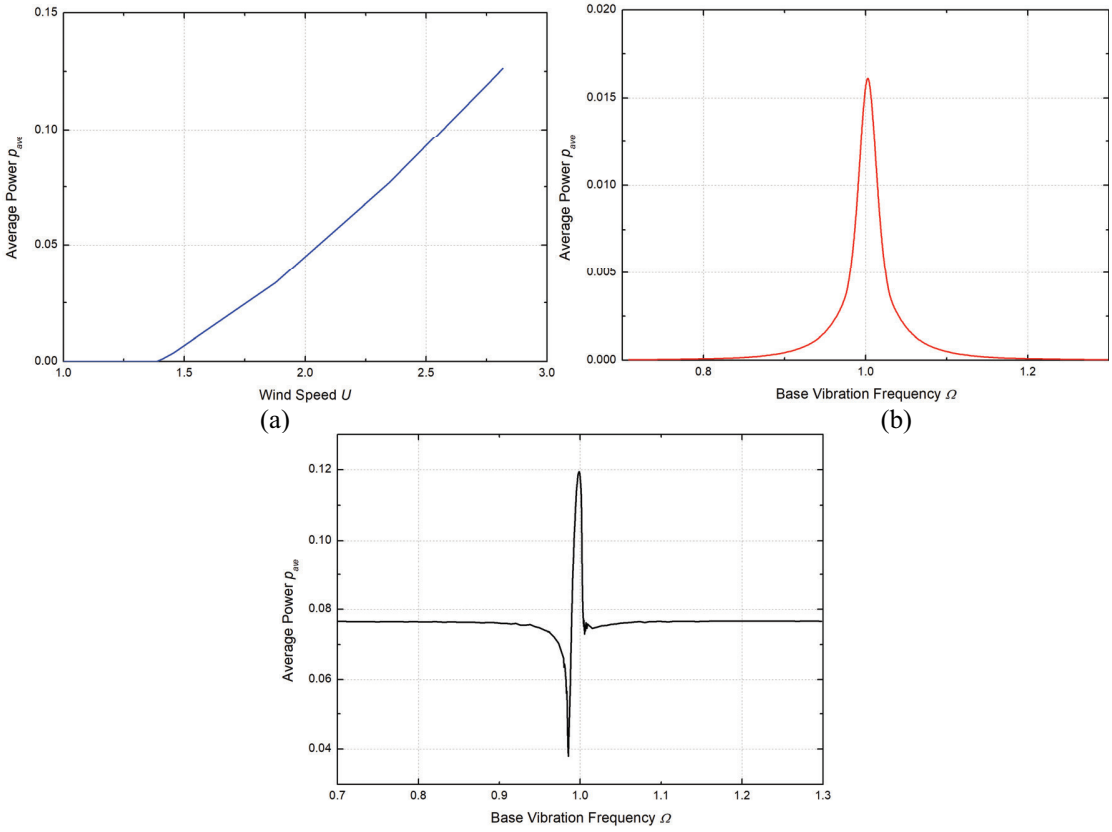

Figure 3. Responses of the original linear galloping energy harvester under (a) pure galloping, (b) pure base vibration and (c) concurrent wind and base vibration excitations

A further look at the time domain displacement response for the linear harvester is shown in Figure 4 (a). At Ω=0.932, it is seen that the response is quasi-periodic with an amplitude modulation frequency under the coupling of two concurrent excitation frequencies. Using a nonlinear bistable configuration with k_1=-0.5 and k_3=3.5, it can be seen from Figure 4(b) that periodic oscillations are achieved where wind and base vibration excitations are locked in. Moreover, the oscillation amplitude of the proposed design is higher than the peak vibration amplitude of the linear counterpart.

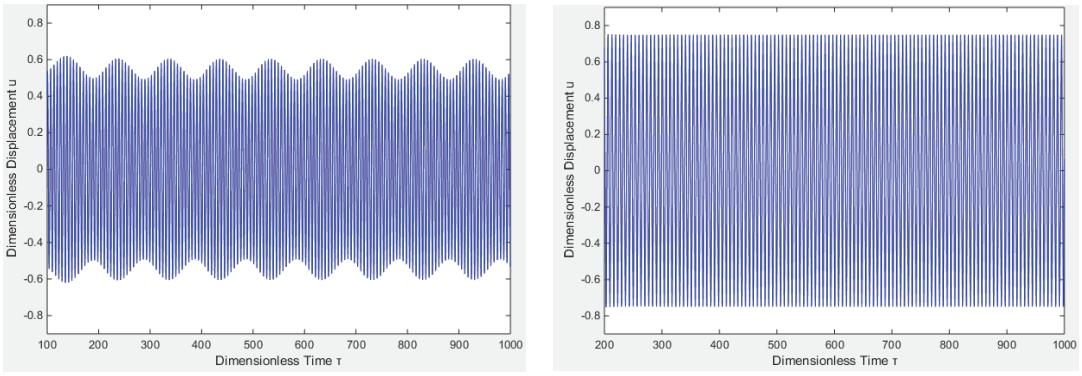

(a) (b)

Figure 4. Time domain dimensionless displacement at Ω=0.932, U=2.347 and a_{rms}=0.005: (a) linear galloping harvester (b) proposed bistable device

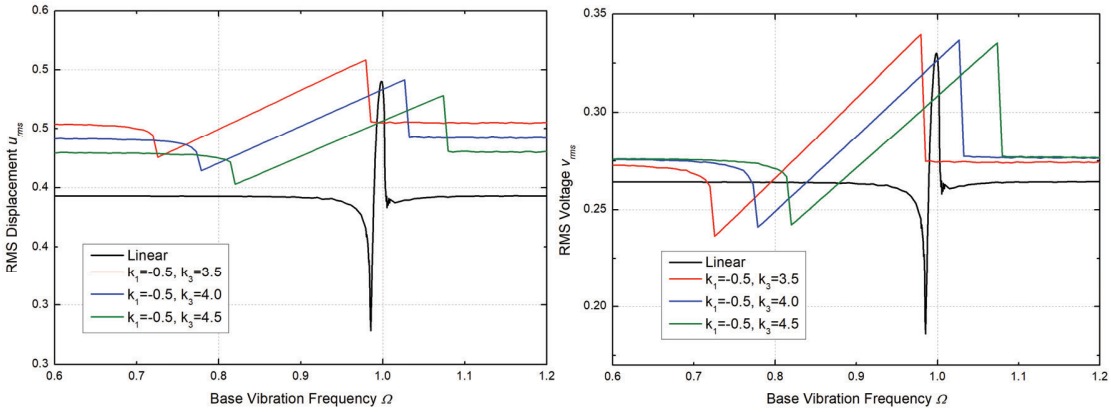

(a) (b)

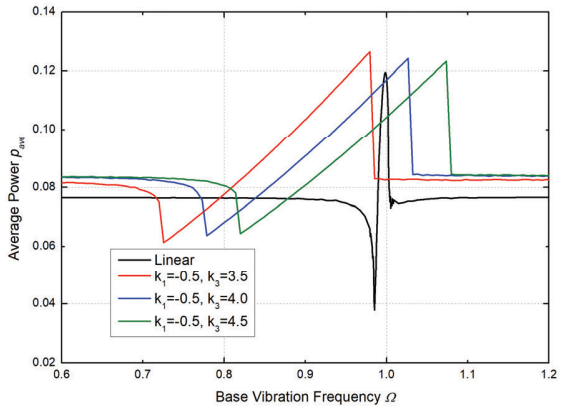

(c)

Figure 5. Variation of (a) u_{rms}, (b) v_{rms} and (c) p_{ave} with Ω for three bistable configurations under concurrent wind and base vibration excitations

The variations of dimensionless RMS displacement u_{rms}, dimensionless RMS voltage v_{rms} and dimensionless average power p_{ave} with base vibration frequency at U=2.347 and a_{rms}=0.005 are shown in Figure 5. Three nonlinear bistable configurations are considered, with k_1=-0.5 and k_3= [3.5, 4.0, 4.5]. From Figure 5(a), it is observed that over the whole range of the considered frequency, wind and base vibration both contribute to the dynamic responses, with higher u_{rms} than the level from pure galloping. As Ω sweeps up, u_{rms} first keeps constant, then decreases to form a valley. Afterwards, u_{rms} steadily increases over a wide range of Ω until it reaches the peak. u_{rms} drops to the former constant value and the curve reverts to be flat when Ω further increases. With identical k_1, it is found that u_{rms} in the flat regions as well as in the peaks increases with k_3. The range of Ω between the valley and the peak is defined here as the primary bandwidth for concurrent energy harvesting. With various k_3, the similar sizes of primary bandwidth are obtained. These bandwidths shift to lower Ω with the increase of k_3.

Similarly, it is seen from Figure 5(b) that enhanced v_{rms} is achieved over a significantly widened bandwidth where wind and base vibration energy are both effectively harnessed. Similar to u_{rms}, when k_3 increases, the primary bandwidth moves to left. Besides the broadened bandwidth, higher maximum v_{rms} is also observed for all three bistable configurations as compared to the linear harvester. The highest peak of v_{rms} is obtained with k_3=3.5. However, in contrast to u_{rms}, in those flat regions, higher v_{rms} is associated with smaller k_3. The voltage valleys of the bistable designs are much shallower than that of the linear harvester, however, the valley ranges are wider. The responses of p_{ave} in Figure 5(c) show similar trends with v_{rms}, with simultaneous broadened bandwidth and enhanced power amplitude for all three bistable configurations. At the dimensionless power level of 0.085, the bandwidth is increased from 0.0118 with the linear harvester to 0.16 with the bistable design of k_1=-0.5, k_3=4.0, which is an over 12 times increase.

5. Conclusion

This paper investigates using an aeroelastic galloping energy harvester with nonlinear bistability to enhance concurrent wind and base vibration energy harvesting. Significantly widened bandwidth is achieved over which both the two energy sources are effectively harnessed. Moreover, enhanced voltage and power amplitudes are obtained. An over 12 times increase in the effective concurrent energy harvesting bandwidth is reached with k_1=-0.5, k_3=4.0 as compared to a linear galloping harvester.

References

[1] H. D. Akaydin, N. Elvin, and Y. Andreopoulos, "The performance of a self-excited fluidic energy harvester," *Smart Materials and Structures,* vol. 21, no. 2, p. 025007, 2012.

[2] A. Bibo and M. F. Daqaq, "Investigation of concurrent energy harvesting from ambient vibrations and wind using a single piezoelectric generator," *Applied Physics Letters,* vol. 102, no. 24, p. 243904, 2013.

[3] A. Barrero-Gil, G. Alonso, and A. Sanz-Andres, "Energy harvesting from transverse galloping," *Journal of Sound and Vibration,* vol. 329, no. 14, pp. 2873-2883, 2010.

[4] Y. Yang, L. Zhao, and L. Tang, "Comparative study of tip cross-sections for efficient galloping energy harvesting," *Applied Physics Letters,* vol. 102, no. 6, p. 064105, 2013.

[5] A. Abdelkefi, J. M. Scanlon, E. McDowell, and M. R. Hajj, "Performance enhancement of piezoelectric energy harvesters from wake galloping," *Applied Physics Letters,* vol. 103, no. 3, p. 033903, 2013.

[6] G. Hu, K.-T. Tse, K. C. Kwok, J. Song, and Y. Lyu, "Aerodynamic modification to a circular cylinder to enhance the piezoelectric wind energy harvesting," *Applied Physics Letters,* vol. 109, no. 19, p. 193902, 2016.

[7] L. Zhao, L. Tang, and Y. Yang, "Enhanced piezoelectric galloping energy harvesting using 2 degree-of-freedom cut-out cantilever with magnetic interaction," *Japanese Journal of Applied Physics,* vol. 53, no. 6, p. 060302, 2014.

[8] L. Zhao and Y. Yang, "Enhanced aeroelastic energy harvesting with a beam stiffener," *Smart Materials and Structures,* vol. 24, no. 3, p. 032001, 2015.
[9] L. Zhao, L. Tang, J. Liang, and Y. Yang, "Synergy of wind energy harvesting and synchronized switch harvesting interface circuit," *IEEE/ASME Transactions on Mechatronics,* vol. 22, no. 2, pp. 1093-1103, 2017.
[10] H. L. Dai, A. Abdelkefi, and L. Wang, "Piezoelectric energy harvesting from concurrent vortex-induced vibrations and base excitations," *Nonlinear Dynamics,* vol. 77, no. 3, pp. 967-981, 2014.
[11] A. Bibo, A. Abdelkefi, and M. F. Daqaq, "Modeling and characterization of a piezoelectric energy harvester under Combined Aerodynamic and Base Excitations," *Journal of Vibration and Acoustics,* vol. 137, no. 3, p. 031017, 2015.
[12] R. Harne and K. Wang, "A review of the recent research on vibration energy harvesting via bistable systems," *Smart Materials and Structures,* vol. 22, no. 2, p. 023001, 2013.
[13] S. Zhou, J. Cao, A. Erturk, and J. Lin, "Enhanced broadband piezoelectric energy harvesting using rotatable magnets," *Applied Physics Letters,* vol. 102, no. 17, p. 173901, 2013.
[14] M. Soliman, E. Abdel-Rahman, E. El-Saadany, and R. Mansour, "A wideband vibration-based energy harvester," *Journal of Micromechanics and Microengineering,* vol. 18, no. 11, p. 115021, 2008.
[15] H. Liu, C. J. Tay, C. Quan, T. Kobayashi, and C. Lee, "A scrape-through piezoelectric MEMS energy harvester with frequency broadband and up-conversion behaviors," *Microsystem technologies,* vol. 17, no. 12, pp. 1747-1754, 2011.
[16] L. Zhao and Y. Yang, "An impact-based broadband aeroelastic energy harvester for concurrent wind and base vibration energy harvesting," *Applied Energy,* vol. 212, pp. 233-243, 2018.
[17] L. Zhao, "Performance Enhancement of an Aeroelastic Energy Harvester for Efficient Power Harvesting from Concurrent Wind Flows and Base Vibrations," in *2018 IEEE/ASME International Conference on Advanced Intelligent Mechatronics (AIM)*, Auckland, New Zealand, 2018, pp. 780-785.
[18] J. P. Den Hartog, *Mechanical Vibrations*. New York: McGraw-Hill, 1956.